

Tribological properties of thin films made by atomic layer deposition sliding against silicon

Lauri Kilpi, Oili M. E. Ylivaara, Antti Vaajoki, Xuwen Liu, Ville Rontu, Sakari Sintonen, Eero Haimi, Jari Malm, Markus Bosund, Marko Tuominen, Timo Sajavaara, Harri Lipsanen, Simo-Pekka Hannula, Riikka L. Puurunen, and Helena Ronkainen

Citation: *Journal of Vacuum Science & Technology A* **36**, 01A122 (2018); doi: 10.1116/1.5003729

View online: <https://doi.org/10.1116/1.5003729>

View Table of Contents: <https://avs.scitation.org/toc/jva/36/1>

Published by the [American Vacuum Society](#)

ARTICLES YOU MAY BE INTERESTED IN

Review Article: Recommended reading list of early publications on atomic layer deposition—Outcome of the “Virtual Project on the History of ALD”

Journal of Vacuum Science & Technology A **35**, 010801 (2017); <https://doi.org/10.1116/1.4971389>

Surface chemistry of atomic layer deposition: A case study for the trimethylaluminum/water process

Journal of Applied Physics **97**, 121301 (2005); <https://doi.org/10.1063/1.1940727>

Atomic layer deposition of molybdenum disulfide films using MoF₆ and H₂S

Journal of Vacuum Science & Technology A **36**, 01A125 (2018); <https://doi.org/10.1116/1.5003423>

Atomic layer deposition of AlN from AlCl₃ using NH₃ and Ar/NH₃ plasma


Journal of Vacuum Science & Technology A **36**, 021508 (2018); <https://doi.org/10.1116/1.5003381>

Aluminum oxide/titanium dioxide nanolaminates grown by atomic layer deposition: Growth and mechanical properties

Journal of Vacuum Science & Technology A **35**, 01B105 (2017); <https://doi.org/10.1116/1.4966198>

Crystallinity of inorganic films grown by atomic layer deposition: Overview and general trends


Journal of Applied Physics **113**, 021301 (2013); <https://doi.org/10.1063/1.4757907>



Instruments for Advanced Science

Contact Hiden Analytical for further details:
W www.HidenAnalytical.com
E info@hiden.co.uk

CLICK TO VIEW our product catalogue



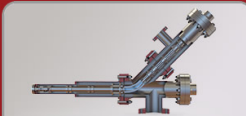
Gas Analysis

- dynamic measurement of reaction gas streams
- catalysis and thermal analysis
- molecular beam studies
- dissolved species probes
- fermentation, environmental and ecological studies




Surface Science

- UHV TPD
- SIMS
- end point detection in ion beam etch
- elemental imaging - surface mapping



Plasma Diagnostics

- plasma source characterization
- etch and deposition process reaction kinetic studies
- analysis of neutral and radical species



Vacuum Analysis

- partial pressure measurement and control of process gases
- reactive sputter process control
- vacuum diagnostics
- vacuum coating process monitoring

Tribological properties of thin films made by atomic layer deposition sliding against silicon

Lauri Kilpi,^{a)} Oili M. E. Ylivaara, and Antti Vaajoki

VTT Technical Research Centre of Finland, Ltd., P.O. Box 1000, FI-02044 VTT, Finland

Xuwen Liu and Ville Rontu

Department of Chemistry and Materials Science, Aalto University School of Chemical Engineering,
P.O. Box 16100, FI-00076 Aalto, Finland

Sakari Sintonen

Department of Electronics and Nanoengineering, Aalto University School of Electrical Engineering,
P.O. Box 13500, FI-00076 Aalto, Finland

Eero Haimi

Department of Chemistry and Materials Science, Aalto University School of Chemical Engineering,
P.O. Box 16100, FI-00076 Aalto, Finland

Jari Malm

Department of Physics, University of Jyväskylä, P.O. Box 35, FI-40014 Jyväskylä, Finland

Markus Bosund

Beneq, Ltd., Ensimmäinen savu, FI-01510 Vantaa, Finland

Marko Tuominen

ASM Microchemistry, Ltd., Pietari Kalmin katu 1 F 2, FI-00560 Helsinki, Finland

Timo Sajavaara

Department of Physics, University of Jyväskylä, P.O. Box 35, FI-40014 Jyväskylä, Finland

Harri Lipsanen

Department of Electronics and Nanoengineering, Aalto University School of Electrical Engineering,
P.O. Box 13500, FI-00076 Aalto, Finland

Simo-Pekka Hannula

Department of Chemistry and Materials Science, Aalto University School of Chemical Engineering,
P.O. Box 16100, FI-00076 Aalto, Finland

Riikka L. Puurunen

Department of Chemical and Metallurgical Engineering, Aalto University School of Chemical Engineering,
P.O. Box 16100, FI-00076 Aalto, Finland and VTT Technical Research Centre of Finland, Ltd.,
P.O. Box 1000, FI-02044 VTT, Finland

Helena Ronkainen

VTT Technical Research Centre of Finland, Ltd., P.O. Box 1000, FI-02044 VTT, Finland

(Received 7 September 2017; accepted 28 November 2017; published 29 December 2017)

Interfacial phenomena, such as adhesion, friction, and wear, can dominate the performance and reliability of microelectromechanical (MEMS) devices. Here, thin films made by atomic layer deposition (ALD) were tested for their tribological properties. Tribological tests were carried out with silicon counterpart sliding against ALD thin films in order to simulate the contacts occurring in the MEMS devices. The counterpart was sliding in a linear reciprocating motion against the ALD films with the total sliding distances of 5 and 20 m. Al₂O₃ and TiO₂ coatings with different deposition temperatures were investigated in addition to Al₂O₃-TiO₂-nanolaminate, TiN, NbN, TiAlCN, a-C:H [diamondlike carbon (DLC)] coatings, and uncoated Si. The formation of the tribolayer in the contact area was the dominating phenomenon for friction and wear performance. Hardness, elastic modulus, and crystallinity of the materials were also investigated. The nitride coatings had the most favorable friction and wear performance of the ALD coatings, yet lower friction coefficient was measured with DLC a-C:H coating. These results help us to take steps toward improved coating solutions in, e.g., MEMS applications. *Published by the AVS.* <https://doi.org/10.1116/1.5003729>

I. INTRODUCTION

Atomic layer deposition (ALD) is a chemical vapor deposition method which allows growth of uniform coatings on complicated 3D geometries.^{1–3} ALD technique is based on

sequential gas–solid reactions that are self-terminating; ALD operates by exposing a solid surface alternately to reactive gaseous chemicals, the exposures being separated by purge/evacuation.^{1–3}

ALD has been developed (under different names) since the 1960s.⁴ One of the main motivations for the recent development of ALD has been semiconductor processing, where the

^{a)}Electronic mail: lauri.kilpi@vtt.fi

miniaturization requires precise thickness control over three dimensional substrates.³ The films deposited by ALD are also used in microelectromechanical system (MEMS) where the major benefit of ALD is the combination of low deposition temperatures (often under 300 °C) with conformal coatings, a combination rarely achieved by conventional coating processes.⁵ The first reports of ALD for MEMS date from a decade ago and dealt with ALD as a tribological coating⁶ and an insulating layer.⁷ Since then, ALD films have been demonstrated, e.g., as dielectric layers in radio frequency (RF) MEMS,⁸ lubricating films,⁹ insulator in MEMS compass,^{10,11} mirrors in Fabry–Perot interferometers for visible light,^{12,13} antistiction layers,¹⁴ and nanoelectromechanical system switches.¹⁵

Single crystal silicon is a highly desirable material for implementing MEMS due to its reliable and reproducible mechanical and electrical properties.¹⁶ Without any constraints the crystal growth direction (111) is favored, providing the highest atomic packing density and also the slowest growth rate of all the possible planes. The (111) oriented silicon slices used to be the standard for the industry, but structures like (100) and (110) have become more and more common lately, especially with the help of beam lead technology and dielectric isolated structures. The crystal orientation of silicon has an effect on certain anisotropic material properties, e.g., elastic modulus, hardness, and etch rate.¹⁷ Also, friction behavior has been reported to change with the different crystal structures of Si.^{18,19}

The performance and reliability of the MEMS devices can be dominated by interfacial phenomena, such as adhesion, friction, and wear.^{6,20,21} Understanding and controlling the friction and wear properties is crucial, especially with moving parts, which can be in contact intentionally or unintentionally during device operation. The friction and wear performance of materials can be studied with various test methods using various contacts, loads, and velocity conditions. Pin-on-disk test is one typical method using a pin sliding against a flat disk. The pin can have different geometries, such as spherical or flat-ended surface. Frictional force is recorded during the experiment and the wear of the pin and the disk are inspected after the experiments, e.g., by microscope or profilometry. Besides the wear of contacting materials, the formation of tribolayers on one or both of the surfaces typically occurs. Earlier studies related to friction and wear of ALD coatings include, e.g., ZnO, WS₂, and Zn_xTi_yO_z with mainly Si₃N₄ used as counterpart.^{22–26} It is also claimed^{27,28} that the ALD Al₂O₃ coating deposited at 50 °C does not form a tribolayer during sliding contact resulting in a low friction coefficient.

Diamond-like carbon (DLC) coatings provide low friction and good wear resistance for many practical applications and contact conditions, and the DLC coatings have been under extensive research for decades.^{29–31} Hydrogenated amorphous carbon (a-C:H) type DLC films can provide low friction performance in different atmospheres and with different contact parameters³¹ and they are widely in use. The friction coefficient of a-C:H coatings against steel materials in normal atmosphere is in the range of 0.1 to 0.2 (Ref. 32) and friction measurements against ceramic materials, such as

Al₂O₃ coatings, provide low values, even down to 0.02,³² depending on the test parameters.

The goal of this work is to investigate the tribological properties of conventional and some potential ALD coatings usable in MEMS applications. Since silicon is a widely used substrate material in MEMS and tribological properties of ALD films on silicon are of the interest of this study, we developed the method for simulating the tribological contact between silicon and ALD films under reciprocating sliding. A hemispherical pin fabricated from single crystal silicon was used as a counterpart for ALD films. A DLC (a-C:H) film was used as a reference as the coating provides an excellent reference for the tribological performance also for the ALD films studied in this research. The friction performance of a-C:H against silicon is not well known, and therefore, this study is also broadening the understanding of a-C:H coating behavior in different contact situations.

II. EXPERIMENT

A. Sample preparation

1. Disk samples

As substrates for ALD coatings, single and double side polished 150 mm p-type <100> silicon wafers with thickness of 675 and 380 μm, respectively, were used. Wafers were cleaned before the ALD using standard Radio Corporation of America cleaning baths (SC1, HF, and SC2)³³ as described in earlier publication by Ylivaara *et al.*³⁴ Studied ALD coatings, described in Table I, were aluminum oxide (Al₂O₃), titanium dioxide (TiO₂), Al₂O₃-TiO₂ nanolaminates (later ATO nanolaminate), plasma-enhanced ALD (PEALD) titanium nitride (TiN), niobium nitride (NbN), and titanium aluminum carbonitride (TiAlCN). The different coatings studied are listed in Table I.

Aluminum oxide (Al₂O₃), titanium dioxide (TiO₂), and ATO nanolaminate were deposited in a top-flow Picosun R-150 ALD reactor. Precursors were trimethylaluminum (Me₃Al), titanium tetrachloride (TiCl₄), and water (H₂O). Electronic grade Me₃Al and TiCl₄ precursors were from SAFC Hitech. Nitrogen (purity > 99.999%) was used both as a purge gas and for flushing the reactant lines with a constant 200 sccm flow. The intermediate space pressure in the reactor was about 700 Pa. Me₃Al and TiCl₄ precursors were cooled with a Peltier element to about 17 and 14 °C, respectively. Water was used at a room temperature without cooling. ALD Al₂O₃ and TiO₂ samples were deposited using 0.1–4.0–0.1–4.0 s pulse sequence for metal precursor pulse–purge–H₂O pulse–purge at a temperature range from 110 to 200 °C. For Al₂O₃ and TiO₂ samples deposited at 300 °C, shorter pulse sequence was used, namely, 0.1–1.0–0.1–1.0 s for metal precursor pulse–purge–H₂O pulse–purge. Targeted layer thicknesses were 100 and 300 nm for Al₂O₃, and 100 nm for TiO₂ coatings. In ATO nanolaminate targeted total thickness was 100 nm with about 5 nm bilayer thickness (composed of 2 nm Al₂O₃ and 3 nm TiO₂ sublayers) as described in Ref. 35. Targeted TiO₂ content in the nanolaminate was 60%. ATO nanolaminate was deposited at 200 °C from sequential Al₂O₃ and TiO₂ layers, using pulse sequence with 4.0 s purges. The structure of the nanolaminate started

TABLE I. Summary of the samples evaluated for tribological properties in this work.

Coating	Target coating thickness (nm)	Deposition temperature (°C)
Si reference sample	—	—
Al ₂ O ₃ low temperature	100	50
Al ₂ O ₃ temperature series	300	110, 150, 200, 250, 300
TiO ₂ temperature series	100	110, 150, 200, 250, 300
ATO temperature series	100	110, 150, 200, 250, 300
TiN	100	300
NbN	100	400
TiAlCN	100	400
DLC	85	200

with Al₂O₃ layer followed by the TiO₂. The total nanolaminate structure was capped with an about 2 nm in thickness Al₂O₃ layer.

Low-temperature ALD Al₂O₃ film was grown at 50 °C in a Beneq TFS 200 ALD reactor at 150 Pa pressure. Precursors (Me₃Al and H₂O) were evaporated by means of their own vapor pressure from external precursor bottles kept at 20 °C. Electronic grade Me₃Al precursor was from SAFC Hitech. Nitrogen was used as the purge gas and it was generated from compressed particle-free dry air by an Inmatec PN-1150 molecular sieve nitrogen separator (purity > 99.999%). The precursor pulses were kept at 0.15 s and the purge periods following the Me₃Al/H₂O precursor pulse was 7 and 20 s. The number of deposition cycles was aimed at a 100 nm film thickness.

ALD TiAlCN films were grown in ASM's EmerALD[®] showerhead single-wafer ALD reactor using TiCl₄ (Sigma-Aldrich 99.9%), Me₃Al (SAFC Hitech Electronic grade) and ammonia (NH₃) (AGA 5.0 with purifier) as precursors and nitrogen (AGA High Tech with purifier) as carrier and purge gas. The precursors were kept at room temperature of about 21 °C.

PEALD TiN layers were grown in a Beneq TFS 200. Precursor purity was 99.999% or better. Nitrogen was used as the carrier gas. Titanium tetrachloride (TiCl₄) and ammonia plasma were used as the precursors. The reactor temperature was 300 °C.

Niobium nitride (NbN) thin films were grown as described in Ref. 36 in a top-flow Picosun R-200 ALD reactor equipped with a load-lock. Precursors used were research grade niobium pentachloride (NbCl₅) (SAFC Hitech) and NH₃ (purity > 99.999%) with nitrogen as the carrier gas. As substrate, 300 μm thick 100 mm p-type ⟨100⟩ Si wafer was used, cleaned with SC1 and HF. Deposition was carried out at 400 °C using 1.5–5.0 and 1.0–6.0 s pulse–purge sequence for NbN and NH₃, respectively. The number of deposition cycles used were 3600, aiming for 100 nm film thickness.

The DLC coatings were deposited for this study with the capacitively coupled RF plasma device with a plasma enhanced chemical vapor deposition method. The substrates were placed directly on the powered cathode, and methane (CH₄) was used as the source gas to deposit amorphous hydrogenated (a-C:H) coatings on silicon wafer. Prior to deposition, the substrates were sputter cleaned in argon

plasma. The pressure was 6 Pa and the bias voltage –500 V during the deposition. The deposition temperature was about 200 °C, and the growth rate of the coating was 0.5 μm/h. The final coating thickness was 85 nm. The DLC films were used as the reference coating for the ALD films.

2. Pin samples

The pin samples were attached on 8 mm thick aluminum disks (Al 6082, diameter 40 mm) using glue (Henkel's Loctite 401) to ensure firm fastening in the test device. Different glues were compared and the selected one provided the most stable performance with no effects on the silicon system under increasing load. The counter surface was a pin with a top part fabricated of bulk single crystal silicon. The surface of the silicon part, presented in Fig. 1 with disk sample, was hemispherical with a 50 mm radius of curvature; it was polished to mirror finish and cleaned before testing with petroleum ether, ethanol and acetone. The indentation hardness and modulus, measured using the microcombi tester (MCT), were $H_{IT} = 9.8 \pm 0.7$ GPa and $E_{IT} = 202 \pm 15$ GPa, respectively. The arithmetic average surface roughness of the Si pin contact surface, measured using Mitutoyo Formtracer SV-C-3100 2D-profilometry, was $R_a = 0.004 \pm 0.001$ μm.

B. Coating characterization

1. XRR

The thickness values of the ALD films were determined by x-ray reflectivity (XRR).^{37,38} In XRR, x-rays are specularly reflected from interfaces of materials with different electron densities, and the influence of layer thicknesses on the reflected x-ray intensity may be recursively calculated as a function of scattering angle.³⁹ The XRR measurements were performed under parallel beam conditions using a Philips X'Pert Pro diffractometer. The acceleration voltage, anode current, and x-ray wavelength were 40 kV, 40 mA, and Cu-K_α, respectively. The film thickness values were obtained through simulation of XRR measurement curves using the software X'PERT REFLECTIVITY.

2. GIXRD

Grazing incidence x-ray diffraction (GIXRD) was used to study the crystallinity of the samples. In GIXRD, the incident angle is set to a small value slightly larger than the critical

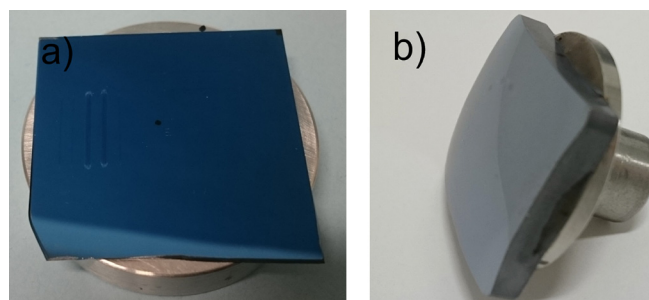


Fig. 1. (Color online) Samples used in the experiments: (a) ALD coated Si wafer glued on the Al disk with the wear tracks of reciprocating sliding tests shown on the surface, and (b) the pin with a hemispherical silicon top part.

angle of total external reflection. The incident angle is kept constant during the measurement, while the scattering angle is scanned. Thanks to the small incident angle, GIXRD probes a much larger volume than conventional powder diffraction, enabling diffraction to be recorded from films with thicknesses of only a few tens of nanometers. The GIXRD experiments were conducted using the same parallel beam setup and conditions as the XRR measurements. The incident angle was fixed at $\omega = 0.5^\circ$.

3. Nanoindentation

Nanoindentation measurements were carried out with a Hysitron TriboIndenter[®] TI-900 nanomechanical testing system. Measurements were done in a semiclean room with constant laminar airflow to minimize the possible thermal drift during the measurements. Indentations were performed under load-control mode with the loading, holding at peak-load and unloading segment times of 10, 5, and 5 s, respectively.

A cube-corner indenter with a 90° total induced angle and a tip radius under 40 nm was used in the study. The purpose of using a sharp tip was to trigger plastic deformation at shallow indents, less than 10% of the film thickness, in order to measure the film hardness with minimal substrate effects.

The mechanical properties of the indented material were extracted from a series of load and depth data using the Oliver and Pharr method,⁴⁰ where the elastic modulus of the film E_f and the diamond tip, E_i are related to the contact modulus, E^* , through the following equation:

$$\frac{1}{E^*} = \frac{1 - \nu_i^2}{E_i} + \frac{1 - \nu_f^2}{E_f}, \quad (1)$$

where ν_i and ν_f are the Poisson's ratio for the diamond tip and grown film (or the Si reference), respectively. For the diamond tip, 1140 GPa and 0.07 were used for E_i and ν_i , respectively. Poisson's ratio of $\nu_f = 0.24$ (Ref. 41) was used for the Al_2O_3 , 0.28 for TiO_2 ,⁴² 0.30 for NbN,⁴³ 0.23 for PEALD TiN (Ref. 44) films, and 0.25 for silicon. For ATO nanolaminate and TiAlCN coatings, contact modulus value are calculated instead. Reference values⁴⁵ are given in a wide range for Poisson's ratios of Si, 0.048–0.403, due to the anisotropic nature of Si. The average value used in this study should be reasonable considering the orientation of Si in our case. The hardness of the film is defined as the maximum indentation load divided by the contact area corresponding to the load⁴⁶

$$H = \frac{P_{\max}}{A}. \quad (2)$$

The instrument stability and indentation repeatability were monitored by performing a series of 16 indents into a piece of silicon wafer over a period of time with the peak load varying from 5 to 500 μN . The silicon reference sample was taken from the same wafer batch that was used as the substrate for the Al_2O_3 films. The indenter conditions (tip rounding) were also checked throughout the measurement

by indenting on the standard fused quartz to see the need of the tip area function for recalibration.

C. Tribological testing

Tribological tests were designed to simulate the contact conditions occurring in MEMS. The MCT (Anton Paar Tritec) and pin-on-disk tribometer (tribometer 1) (Anton Paar Tritec) were used for friction and wear evaluation in reciprocating motion. The silicon pin was rotated to provide new contact surface for each test. Therefore, the crystal orientation varied between the tests, which might have caused some variation in the friction performance of the coatings.

1. Stepwise reciprocative sliding

The Si pin was sliding back and forth against the coated wafers with a constant load to perform the reciprocating sliding motion. The constant load of 300 mN was used during the tests, the sliding speed was 0.01 m s^{-1} , and the length of the sliding pass in one direction was 10 mm. In the tests carried out with the MCT, the movement was stopped for about 1 s after each sliding pass before sliding to opposite direction. The testing was carried out stepwise manner using five steps. During each step, the Si pin was sliding the selected number of passes on the coated disk after which optical microscopy (OM) was used to investigate the status of the coating. Optical microscopy was used after the steps of 50, 100, 200, 300, and 500 sliding passes which formed the basic routine. The sliding distance of 500 passes generated the total sliding distance of 5 m. The coatings that showed low wear were tested with 500 extra passes after the basic test routine. During the tests friction force was measured to determine the friction coefficient. For the tests carried out in stepwise manner using the MCT device, the average friction values were determined for the 1st, 100th, 200th, 300th, 400th, and 500th sliding pass as the mean value of one sliding cycle representing the friction performance.

2. Continuous reciprocative sliding

The materials with high friction performance were selected for further studies. The continuous reciprocating sliding tests were carried out for selected samples with the tribometer 1 using the sliding distances of 5 m (500 cycles) and 20 m (2000 cycles) in order to compare the long term performance of coatings. The constant load was 300 mN, the sliding speed was 0.01 m s^{-1} , and the length of the sliding pass in one direction was 10 mm as in previous tests. In this test procedure, the sliding was continuous without pauses between the 10 mm unidirectional sliding cycles before the change in direction. In these continuous reciprocating sliding tests, recorded friction data had either a positive or negative sign, depending on the sliding direction. Here for clarity, the absolute values were combined to create the continuous friction curves shown in this paper. Moving average (consisting of 1000 points) was also created and plotted in the friction graphs. Two to three repeated tests were carried out for all the coatings, and the experiments were carried out in the

TABLE II. Thickness, deposition temperature, hardness, elastic modulus, and crystallinity of the ALD coatings studied.

ALD films	Temperature (°C)	Thickness (nm)	Hardness (GPa)	Elastic modulus (GPa)	Crystallinity
Si reference	—	—	—	—	—
Al ₂ O ₃	50	98	6.1 ± 0.3	135 ± 27	Amorphous
Al ₂ O ₃	110	288 ^a	7.9 ± 0.2 ^a	139 ± 9 ^a	Amorphous
Al ₂ O ₃	150	285 ^a	10.0 ± 0.2 ^a	171 ± 12 ^a	Amorphous
Al ₂ O ₃	200	287 ^a	9.8 ± 0.3 ^a	167 ± 11 ^a	Amorphous
Al ₂ O ₃	250	292 ^a	11.1 ± 0.7 ^a	178 ± 15 ^a	Amorphous
Al ₂ O ₃	300	284 ^a	10.5 ± 0.6 ^a	170 ± 10 ^a	Amorphous
TiO ₂	110	97	6.9 ± 0.1	152 ± 5	Amorphous
TiO ₂	150	103	7.3 ± 0.1	149 ± 4	Amorphous
TiO ₂	200	91	8.5 ± 1.0	154 ± 9	Anatase
TiO ₂	250	105	10.5 ± 0.8	159 ± 7	Anatase
TiO ₂	300	104	11.3 ± 1.9	196 ± 30	Anatase
ATO	110	101 ^b	6.8 ± 0.4 ^b	140 ± 12 ^b	Amorphous
ATO	150	103 ^b	7.4 ± 0.2 ^b	147 ± 5 ^b	Amorphous
ATO	200	99 ^b	7.3 ± 0.4 ^b	147 ± 8 ^b	Amorphous
ATO	250	84 ^b	8.2 ± 0.2 ^b	155 ± 9 ^b	Amorphous
ATO	300	84 ^b	8.6 ± 0.2 ^b	156 ± 5 ^b	Amorphous
PEALD TiN	300	116	18.9 ± 0.9	186 ± 33	Rock salt
TiAlCN	400	65	10.8 ± 0.5	125 ± 6	Amorphous
NbN	400	106	19.3 ± 0.7	201 ± 7	Tetragonal

^aValues from Ref. 34.

^bValues from Ref. 35.

controlled environment with temperature 22 ± 1 °C and relative humidity $50 \pm 5\%$ RH.

3. Microscopy and profilometry

After the experiments, OM was used to investigate the wear tracks of both the pin and the disk. The 3D profilometry (Sensofar Plμ 2300) was used to characterize the wear surfaces and 2D profilometry (Mitutoyo Formtracer SV-C3100H4) to determine the volumes of the coating wear. To determine the wear volumes of the coatings, the 2D profiles were taken across the wear track in three locations. The wear of the silicon pin was determined based on the OM of the wear surface. The wear rates were calculated by dividing the wear volumes by load and sliding distance. Selected samples were also analyzed by using scanning electron microscopy (SEM) with energy-dispersive x-ray spectroscopy (EDS) (FEI XL 30 ESEM). EDS analysis was carried out with 15 kV accelerating voltage.

III. RESULTS

A. Coating characteristics

The coating hardness and Young's modulus values obtained by nanoindentation are presented in Table II, presenting also the crystallinity and the coating thickness values characterized by x-ray reflectivity. ALD NbN and PEALD TiN have clearly higher hardness values than the rest of the materials. Most of the ALD films were amorphous, but PEALD TiN, NbN, and the TiO₂ films deposited at temperatures 200 °C and higher, showed crystal structure in GIXRD

measurements (Fig. 2). Since GIXRD measurements measure randomly oriented grains, the high peak intensities of TiO₂ and NbN films suggest no preferred orientation in the films. The lower peak intensity of TiN films on the other hand is probably related to a lower fraction of crystalline material or lower quality of the crystalline structure. The lower density of 6.65 g/cm^3 of the ALD-NbN, as measured by XRR, compared with the tabulated value of 8.47 g/cm^3 of crystalline NbN supports this conclusion. The crystalline TiO₂ films showed anatase phase with increased the surface roughness of the TiO₂ film, particularly for the film deposited at 300 °C.

B. Friction performance of ALD coatings

The friction coefficient values measured in the reciprocating sliding tests with Si pins acting as the counter material against the ALD coatings are listed in Table III representing the values after 0.01, 1, 5, and 20 m sliding.

1. Stepwise reciprocative sliding tests

a. Al₂O₃. The ALD Al₂O₃ coatings deposited in different temperatures had low friction coefficient around 0.2 to 0.3 in the beginning of the test but after some sliding the friction increased to values in the range 0.4 to 0.6, as shown in Table III and Fig. 3(a). The coatings grown at temperatures 110, 150, and 250 °C provided low friction performance for longer sliding distance than the other Al₂O₃ films. During the tests the friction increased also for these coatings reaching values around 0.5 in the end of the test. The Al₂O₃ coating that was deposited in the different reactor at 50 °C temperature had friction values similar to films deposited at 200 and 300 °C.

A typical feature for the Al₂O₃ films was the formation of a tribolayer on the sliding surface of the coating during the sliding tests as shown in Figs. 4(a) and 4(b). The Si pin experienced a noticeable amount of wear, as shown in Fig. 4(c). The increase in friction was most likely related to the formation of tribolayer on the sliding surface of the Al₂O₃ film since the tribolayer consisted of the worn and oxidized

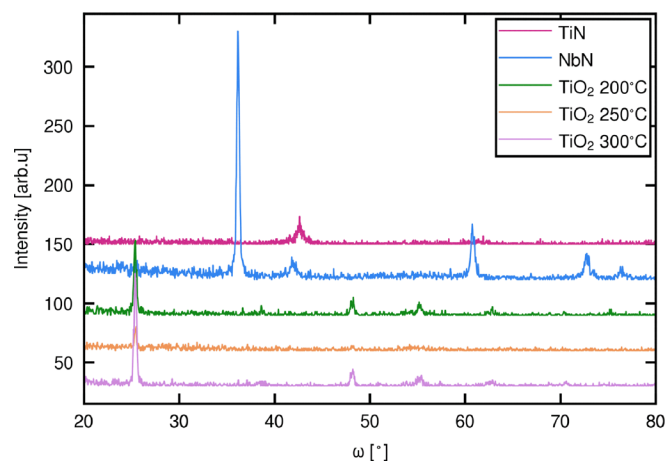


Fig. 2. (Color online) GIXRD graphs of all the crystalline samples: PEALD TiN (100 nm/300 °C), ALD NbN (100 nm/400 °C), ALD TiO₂ (100 nm/200 °C), ALD TiO₂ (100 nm/250 °C) and ALD TiO₂ (100 nm/300 °C).

TABLE III. Friction coefficient values of ALD coatings against silicon pin measured in reciprocative sliding tests with the two test procedures (stepwise sliding and continuous sliding). The average values from at least two repeated tests represent the friction measured after sliding distances of 0.01, 1, 5, and 20 m. The scatter of the results is shown as standard deviation.

Coating	Temperature (°C)	Thickness (nm)	Reciprocative stepwise sliding			Continuous reciprocative sliding			
			μ (0.01 m)	μ (1 m)	μ (5 m)	μ (0.01 m)	μ (1 m)	μ (5 m)	μ (20 m)
Si reference	—	—	0.22 ± 0.10	0.71 ± 0.07	0.70 ± 0.06	0.24 ± 0.09	0.51 ± 0.10	0.55 ± 0.09	—
Al ₂ O ₃	50	98	0.19 ± 0.07	0.45 ± 0.22	0.63 ± 0.10	0.21 ± 0.05	0.39 ± 0.13	0.48 ± 0.11	—
Al ₂ O ₃	110	288 ^a	0.28 ± 0.08	0.21 ± 0.06	0.52 ± 0.11	—	—	—	—
Al ₂ O ₃	150	285 ^a	0.21 ± 0.06	0.21 ± 0.08	0.43 ± 0.09	—	—	—	—
Al ₂ O ₃	200	287 ^a	0.26 ± 0.05	0.61 ± 0.08	0.48 ± 0.09	—	—	—	—
Al ₂ O ₃	250	292 ^a	0.23 ± 0.05	0.20 ± 0.05	0.50 ± 0.08	—	—	—	—
Al ₂ O ₃	300	284 ^a	0.23 ± 0.07	0.45 ± 0.07	0.53 ± 0.08	0.25 ± 0.05	0.25 ± 0.05	0.49 ± 0.08	—
TiO ₂	110	97	0.26 ± 0.08	0.24 ± 0.08	0.33 ± 0.07	0.26 ± 0.12	0.24 ± 0.05	0.43 ± 0.16	—
TiO ₂	150	103	0.43 ± 0.10	0.50 ± 0.13	0.69 ± 0.06	—	—	—	—
TiO ₂	200	91	0.56 ± 0.10	0.65 ± 0.07	0.65 ± 0.07	—	—	—	—
TiO ₂	250	105	0.68 ± 0.11	0.56 ± 0.10	0.51 ± 0.08	—	—	—	—
TiO ₂	300	104	0.67 ± 0.13	0.66 ± 0.10	0.60 ± 0.12	0.71 ± 0.26	0.63 ± 0.10	0.55 ± 0.08	—
ATO	110	101 ^b	0.24 ± 0.05	0.22 ± 0.07	0.25 ± 0.06	—	—	—	—
ATO	150	103 ^b	0.22 ± 0.06	0.21 ± 0.06	0.44 ± 0.10	0.25 ± 0.05	0.19 ± 0.04	0.26 ± 0.10	0.53 ± 0.07
ATO	200	99 ^b	0.20 ± 0.05	0.21 ± 0.06	0.17 ± 0.08	—	—	—	—
ATO	250	84 ^b	0.20 ± 0.04	0.28 ± 0.06	0.49 ± 0.16	0.24 ± 0.04	0.19 ± 0.03	0.43 ± 0.10	—
ATO	300	84 ^b	0.33 ± 0.06	0.19 ± 0.09	0.26 ± 0.07	—	—	—	—
PEALD TiN	300	116	0.51 ± 0.17	0.29 ± 0.07	0.34 ± 0.07	0.78 ± 0.30	0.24 ± 0.07	0.27 ± 0.07	0.30 ± 0.05
TiAlCN	400	65	0.28 ± 0.07	0.35 ± 0.07	0.32 ± 0.08	0.28 ± 0.05	0.28 ± 0.06	0.36 ± 0.06	0.44 ± 0.08
NbN	400	106	0.29 ± 0.09	0.33 ± 0.08	0.36 ± 0.08	0.31 ± 0.08	0.20 ± 0.04	0.30 ± 0.05	0.33 ± 0.03
DLC reference	200	85	—	—	—	0.22 ± 0.13	0.13 ± 0.04	0.12 ± 0.05	—

^aValues from Ref. 34.

^bValues from Ref. 35.

silicon and the sliding thus occurred between similar materials. Sliding between similar materials is known to increase the friction between the surfaces.⁴⁷

b. TiO₂. The friction performance of ALD TiO₂ on Si wafers grown at different temperatures is presented in Fig. 3(b). The friction of TiO₂ was high (0.4–0.7) already in the beginning of the tests for TiO₂ grown at 150 to 300 °C compared to amorphous TiO₂ sample deposited at 110 °C. The friction values was stabilized between 0.50 and 0.70. The TiO₂ coating grown at 110 °C had an exceptionally low friction value of 0.2–0.4 throughout the test.

The TiO₂ coatings deposited at higher temperatures had high friction values (0.5–0.7), and formation of tribolayer on the coating wear track was observed, as can be seen in Fig. 5(a). The tribolayer formation was similar as observed for

Al₂O₃ films. On the other hand, as can be observed in Fig. 5(b), no tribolayer was generated on the TiO₂ grown at 110 °C which had low friction in the tests. The Si pin suffered a noticeable amount of wear in all cases except when sliding against the coating deposited at 110 °C.

c. Al₂O₃-TiO₂ nanolaminates. The results of the ALD ATO nanolaminate coatings deposited at temperatures 110, 200 and 300 °C showed generally low friction values, in the range 0.20 to 0.30, from start to finish. For the coatings deposited at 150 and 250 °C, the friction values increased close to 0.50 during the 500 sliding passes (5 m sliding) test as presented in Fig. 3(c). The coatings with low friction had a smooth wear track without tribolayer formation as observed in Fig. 6(a). On the other hand, pin wear surface showed some layer formation visible in Fig. 6(b). For the

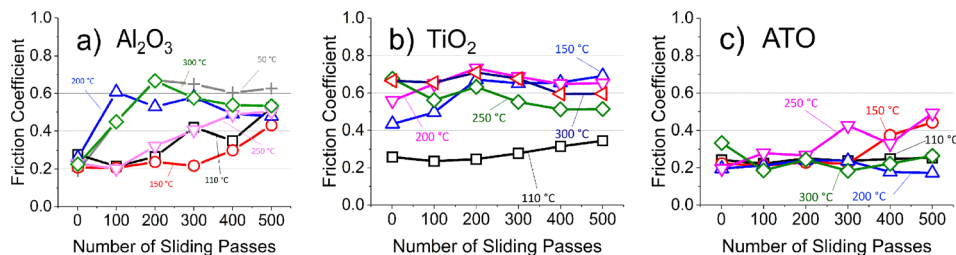


FIG. 3. (Color online) Friction of Al₂O₃, TiO₂ and ATO: The friction coefficient of ALD deposited at different temperatures: (a) Al₂O₃ films (300 nm thick except 100 nm and 50 °C sample), (b) TiO₂ films (100 nm thick) and (c) ATO nanolaminate coatings (100 nm thick). The friction was determined in reciprocative sliding tests carried out in stepwise manner with MCT test device with the 0.3 N normal load, 0.01 m s⁻¹ sliding speed and 500 sliding passes for a total of 5 m sliding distance.

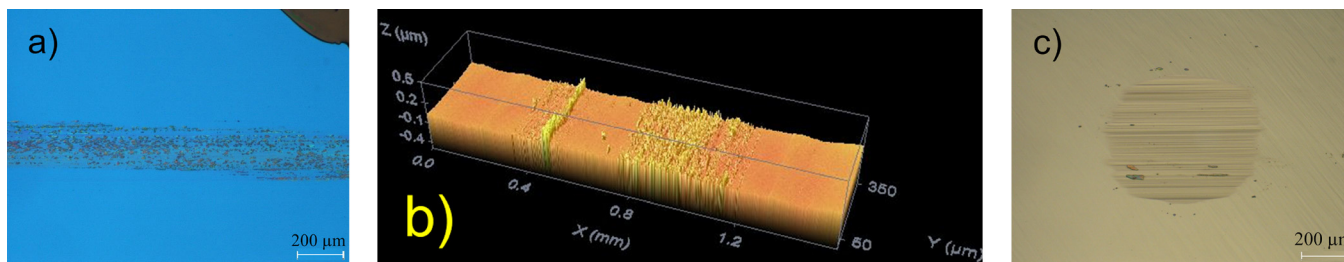


Fig. 4. (Color online) Wear surfaces of Al_2O_3 and Si: (a) The wear track on the ALD Al_2O_3 film (300 nm thick, deposition temperature 300°C), (b) the 3D profile of the wear track on the Al_2O_3 film, and (c) the wear surface of the silicon pin sliding against ALD Al_2O_3 film after the reciprocating sliding test. The reciprocative sliding test was carried out with 0.3 N normal load, 0.01 m s^{-1} sliding speed and 500 sliding passes equivalent to 5 m sliding distance.

ATO films providing higher friction, generation of tribolayer on the coating surface and wear of silicon pin was observed.

2. Continuous reciprocative sliding tests

a. Tests with 5 m sliding distance. Selected samples were tested also for long-term durability and tribological performance with continuous reciprocating sliding tests. These tests were carried out with the tribometer 1 device which provided more accurate friction data as compared to MCT device when low normal loads were used. The friction coefficients, with Si pins acting as the counter material against the ALD coatings, are presented in Table III for 0.01, 1, and 5 m sliding. For the coatings providing low friction in the 5 m sliding tests, also longer 20 m sliding tests were carried out.

The friction evolution graphs from the continuous sliding tests of Al_2O_3 , TiO_2 , ATO, DLC, and uncoated silicon reference are shown in Figs. 7(a)–7(d). The friction of Al_2O_3 deposited at 50 and 300°C was low in the beginning of the test, but increased during the test reaching friction values around 0.5 [Fig. 7(a)]. This performance was comparable to previously presented data obtained from stepwise reciprocating sliding tests. The TiO_2 deposited at 110 and 300°C also showed similar trend as compared to data obtained in the stepwise reciprocating sliding tests. TiO_2 deposited at 110°C had low friction up to 3 m sliding, but increased in the end of the test to friction coefficient value of 0.45 [Fig. 7(b)]. TiO_2 deposited at 300°C had high friction during the whole test duration. The ATO films deposited at 110 and 250°C provided low friction performance with some

variation [Fig. 7(c)]. Also, in the case of 250°C ATO, friction coefficient increased to 0.45 in the end of 5 m sliding.

The friction data of the reference measurements, silicon pin sliding against uncoated (100) silicon wafer and DLC (a-C:H) coated silicon, are presented as reference [Fig. 7(d)]. The reference silicon wafer had low values of about 0.25, which increased and stabilized in the range 0.5 to 0.7 during the 5 m sliding test. A noticeable wear of the Si pin was observed during the test. The DLC coating had a stable friction coefficient at a low value of 0.1–0.2. The contact surface of the DLC film was smooth with no visible tribolayer formation. Also, the wear surface of the silicon pin was smooth with low wear. Overall, the DLC reference provided the lowest friction performance of all tests.

b. Tests with 20 m sliding distance. In the continuous sliding tests, the most promising coatings with a low friction coefficient at the end of the test were ATO, TiN, TiAlCN, and NbN. The 20 m sliding tests were carried out for these coatings in order to observe the durability of the coatings in sliding contact. The friction evolution during the 20 m sliding for these four coatings is presented in Fig. 8.

The friction coefficient of ATO was low in the beginning of the 20 m test, but increased after about 5 m sliding to the level of 0.5 [Fig. 8(a)]. The TiN coating provided lower friction coefficient throughout the 20 m sliding in the range 0.2–0.3 [Fig. 8(a)]. The TiAlCN showed friction values between 0.3 and 0.4 from the start until about 10 m sliding. After 10 m sliding, the friction increased close to 0.6. The coating seemed to wear during the test and toward the end of

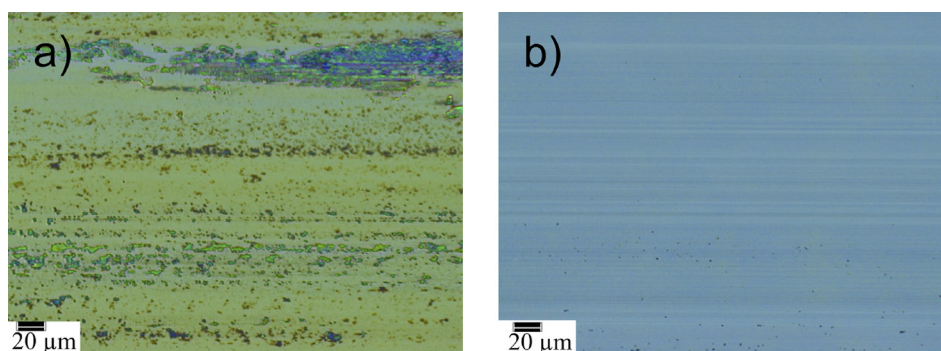


Fig. 5. (Color online) Wear tracks of TiO_2 coating: The wear track on the (a) TiO_2 film (100 nm thick, deposition temperature 300°C) and (b) TiO_2 film (100 nm thick, deposition temperature 110°C). The 0.3 N normal load and 0.01 m s^{-1} sliding speed and 5 m sliding distance was used in the MCT tests.

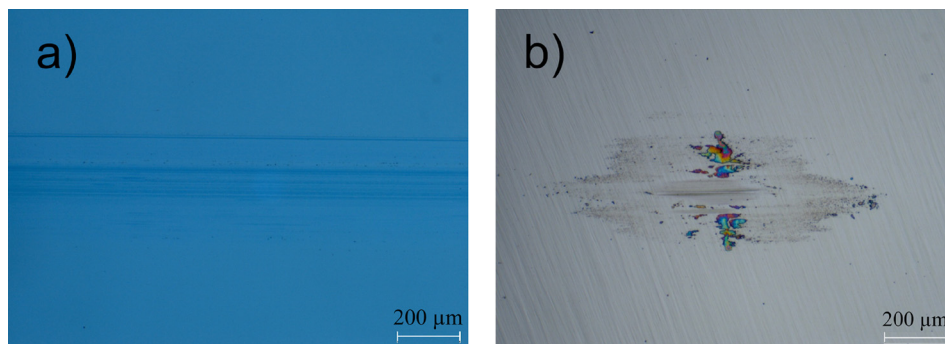


FIG. 6. (Color online) Wear surfaces of ATO and Si: (a) The wear track on the ATO nanolaminate (100 nm thick, deposition temperature 110 °C) and (b) the wear surface of the silicon pin sliding against ATO nanolaminate. The 0.3 N normal load and 0.01 m s⁻¹ sliding speed and 5 m sliding distance was used in the tests.

20 m sliding test, the coating was completely worn through down to the Si substrate [Fig. 9(a)]. As a result, only slight amount of wear was observed on the Si pin. There was a tribolayer formed on top of the Si pin as observed in Fig. 9(b). The tribolayer formed on the Si pin was analyzed by SEM and EDS. The analysis showed that the tribolayer consisted mostly of oxidized coating material accumulated on the sliding surface [Fig. 9(c)]. The friction values of the ALD NbN coating remained low, in the range 0.2–0.4, in the 5 m sliding tests and also throughout the 20 m sliding distance tests. The NbN had more stable friction performance than the PEALD TiN coating. On the NbN surface, no tribolayer was observed [Fig. 10(a)], but the Si pin contact surface had a tribolayer and also loose wear debris around the contact area [Fig. 10(b)]. As a result of the tribolayer, the wear of the Si pin was low.

In Figs. 7 and 8, the actual variation of friction coefficient during the tests is presented combined with the moving average of friction. The variation during tests described the stability of the silicon-coating contact: the lower the variation, the more stable is the tribological performance of the coating against silicon. Considering the friction variation, NbN and TiN showed the most favorable performance in the 20 m test.

C. Wear of ALD films and silicon counterparts

The wear of the silicon pin and of the counterpart was measured after the tests. The results are shown in Table IV. Typically, silicon pin experienced high wear, particularly in the case of Al₂O₃ and TiO₂ coatings. The Si pin wear against ATO films was lower than against Al₂O₃ and TiO₂. The pin

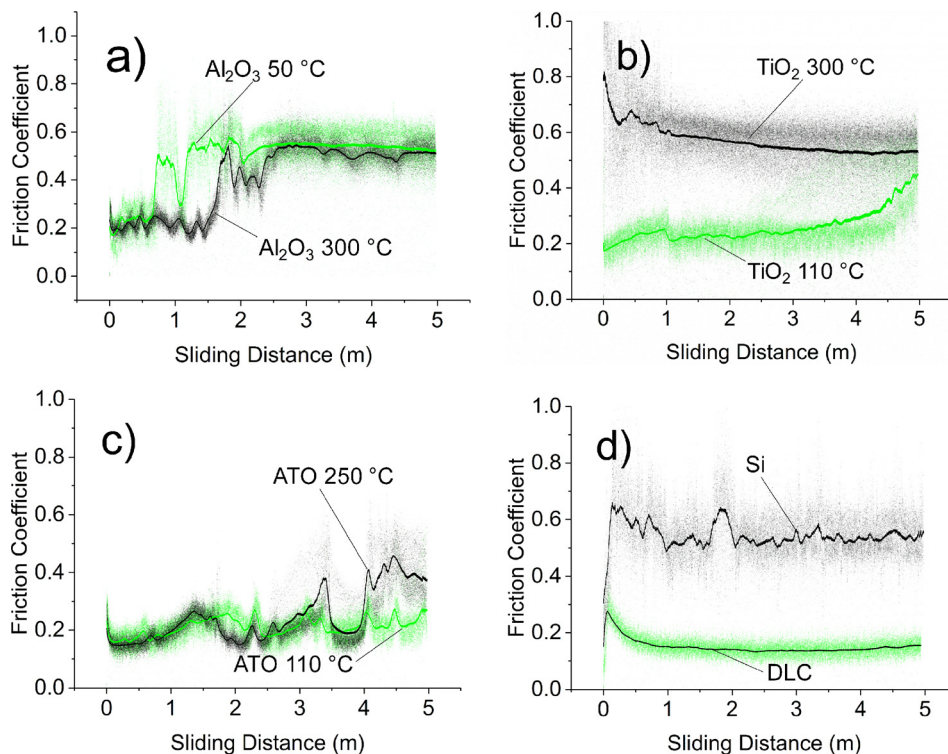


FIG. 7. (Color online) Friction of Al₂O₃, TiO₂, ATO, DLC and Si: The friction coefficient evolution as scatter graphs (with trend line) of continuous reciprocal sliding tests with 0.3 N normal load and 0.01 m s⁻¹ sliding speed with sliding distance of 5 m. (a) ALD Al₂O₃ coatings (100 nm/50 °C and 300 nm/300 °C), (b) ALD TiO₂ coatings (100 nm/300 °C and 100 nm/110 °C), (c) ALD ATO nanolaminate coatings (100 nm/110 °C and 100 nm/250 °C) as well as (d) Si and DLC coatings.

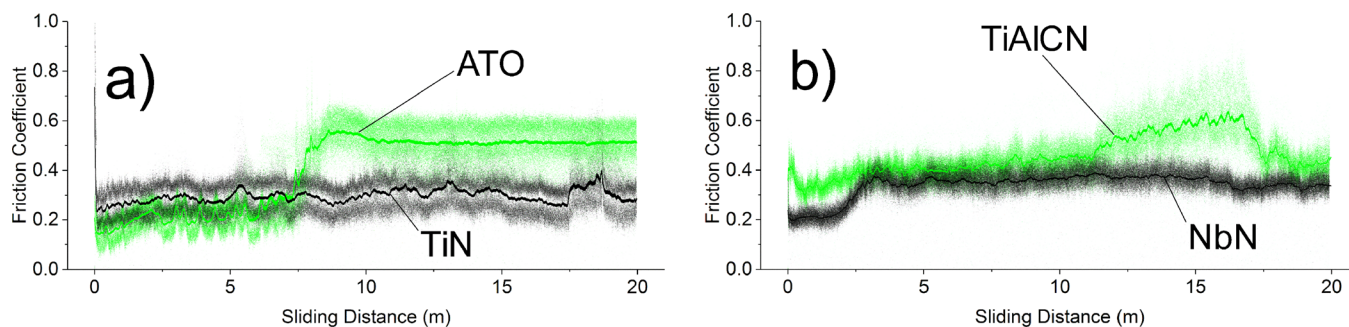


Fig. 8. (Color online) Friction of ATO, TiN, TiAlCN and NbN: The friction coefficient evolution as scatter graphs (with trend line) of continuous reciprocative sliding tests with 0.3 N normal load and 0.01 m s^{-1} sliding speed and sliding distance of 20 m. (a) ALD ATO nanolaminate (100 nm/110 °C) and PEALD TiN coating (100 nm/300 °C), and b) ALD TiAlCN (100 nm/400 °C) and ALD NbN (100 nm/400 °C) coating.

wear against the PEALD TiN, TiAlCN, NbN, and DLC films was below the detection limit.

The wear determination of the ALD films was, in most cases, not possible due to the tribolayer formation or low wear of the coating. The wear rates could be determined for the TiAlCN, NbN, and PEALD TiN films. The TiAlCN had high wear since it was worn throughout the coating [Fig. 9(a)]. The NbN coating had the lowest wear rate [Fig. 10(a)].

IV. DISCUSSION

Friction coefficient is not an intrinsic material parameter but a system parameter. This was clearly observed in the tests carried out with the silicon counter surface sliding against ALD films on silicon. For the friction and wear experiments to succeed, adhesion between Si substrate and the coating needs to be good. For Al_2O_3 , TiO_2 and ATO nanolaminate coatings adhesion was good as described in a previous work.⁴⁸ However, some coating delamination was observed for the PEALD TiN coating during the tests, indicating inadequate adhesion.

The main influencing phenomenon influencing the friction performance was observed to be the tribochemical interaction between silicon and the coating material. Silicon based tribolayer formed on the coating surface generally resulted in a high friction coefficient, such as in Fig. 3 for the Al_2O_3 films and TiO_2 films deposited at high temperatures. The friction increased during sliding up to values 0.5

and even 0.7, which is in the same range as for the silicon against the silicon contact.

The friction and wear values presented in this paper can be compared to other basic tribological contact pairs.⁴⁹ A relatively high friction coefficient is typically generated in dry steel against steel contact, with friction coefficient being in the range from 0.7 to 0.9.⁵⁰ An example of a low friction coefficient value is the contact between DLC and steel with friction coefficient being in the range 0.1–0.2 and even lower values down to 0.002, depending on the coating properties and the test conditions.^{31,32}

For the ALD Al_2O_3 , sliding against silicon, the friction coefficient was about 0.2 in the beginning of the tests but soon increased to values up to 0.5. The increase in friction was connected to the formation of the tribolayer on the wear track of the Al_2O_3 film visible in the 3D profile presented in Fig. 4(b). The tribolayer consisted of oxidized silicon since the silicon pin experienced high wear during the tests. The Al_2O_3 films deposited at temperatures 110, 150, and 250 °C could provide lower friction values for a longer period of sliding compared to films deposited at 200 and 300 °C. As reported earlier by Ylivaara *et al.*,³⁴ the ALD films deposited at low temperatures contain hydrogen which could enhance the low friction performance in the beginning of the test. However, in all cases, the friction increased to values around 0.5 toward the end of the test. High friction and tribolayer formation was also observed in the case of low temperature ALD Al_2O_3 coating deposited at 50 °C, although a published patent²⁸ suggests low friction

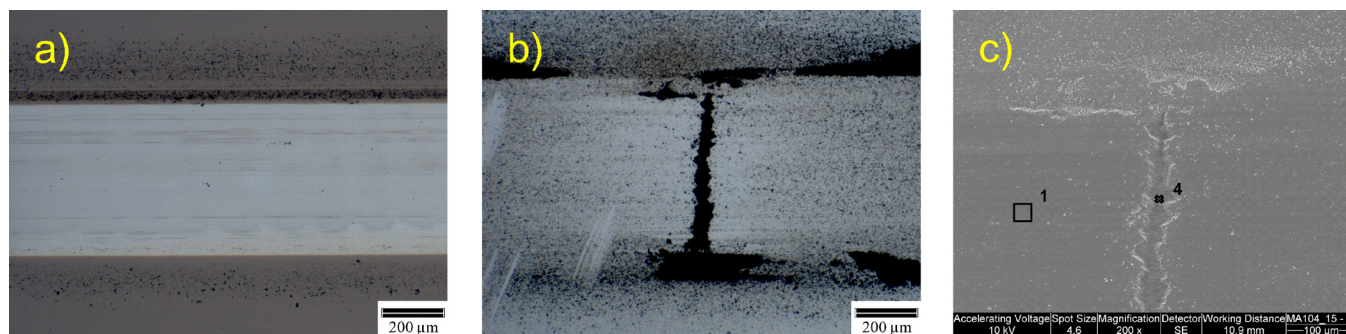


Fig. 9. (Color online) Wear surface of TiAlCN and Si: (a) The wear track on TiAlCN coating (100 nm/400 °C), (b) wear surface of the Si counterpart sliding against TiAlCN, and (c) the SEM image of the wear surface and the tribolayer on the Si pin that was sliding against the TiAlCN coating for 20 m. Point 1 consists of 0.88 (at. %) C, 2.01 O and 97.10 Si. Point 4 consists of 1.44 (at. %) C, 7.52 N, 63.21 O, 0.96 Al, 2.15 Si, 2.12 Cl and 22.60 Ti. The chloride originates as an impurity from the ALD process.

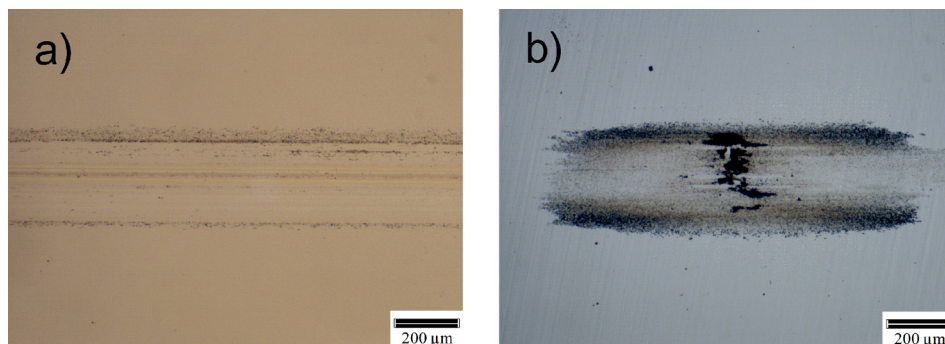


FIG. 10. (Color online) Wear surface of NbN and Si: (a) The wear track on NbN (100 nm/400 °C), and (b) the wear surface of the Si counterpart sliding against NbN after the reciprocative sliding with 0.3 N normal load, sliding velocity of 0.01 m s⁻¹ and sliding distance of 20 m.

performance of such films. Based on the tribological test results, the friction performance of ALD Al₂O₃ films was defined by the tribolayer formation on the coating contact surface and the time required for the tribofilm to evolve.

The deposition temperature of ALD TiO₂ influenced the structure of the coating material, since films deposited at 200 °C and above had a crystalline structure, which increased the surface roughness. The crystallinity and roughness caused the high initial friction values, after which the values leveled down, but still remained between 0.5 and 0.7. ALD TiO₂ deposited at low temperature (110 °C) had amorphous structure providing lower friction performance in the range 0.3 to 0.4. In the sliding tests, only a thin tribolayer was formed on the coating wear track (Fig. 5). According to the results of Ylivaara *et al.*³⁵ concerning TiO₂ and Al₂O₃-TiO₂ nanolaminates, the coatings deposited at low temperature had higher amount of impurities, such as chlorine and hydrogen. Particularly, the hydrogen content might have had a beneficial effect reducing the friction. However, also in this case, the friction was showing an increasing trend toward the end of the 5 m sliding tests. It is noteworthy that the silicon pin wear rate depended on the TiO₂ growth temperature; the higher the temperature, the faster the wear.

When the ALD ATO nanolaminates, consisting of Al₂O₃ and TiO₂ lamellas, were sliding against silicon, little or no tribolayer formed on the surface of the coatings (Fig. 6). Friction was low compared to single material ALD Al₂O₃ and TiO₂ films. In this case, some tribolayer was formed on the contact surface of silicon. The nanolaminate structure, thus, seemed to have a beneficial synergy providing lower friction performance in most cases during the 5 m sliding tests. However, in some cases, the nanolaminate coatings showed increasing values toward the end of the 5 m sliding test and during the 20 m sliding test a tribolayer, increasing the friction coefficient above 0.5, was formed even for the most promising ATO coatings. In the 20 m sliding test, the increase in friction after 5 m is probably due to the bilayer structure of ATO nanolaminate. The outermost 2 nm thick Al₂O₃ layer might have worn out exposing the TiO₂ into the contact.

The ALD coatings prone to generate a tribolayer on the coating surface thus increasing the friction were Al₂O₃, TiO₂, and ATO nanolaminate. The silicon pin was typically worn forming of a tribolayer consisting of silicon oxide on

top of the coating surface. Especially in the case of TiO₂, the wear of Si pin was significant due to the deposition temperature of the coating being 300 °C. The increased deposition temperature caused the TiO₂ to grow as anatase, with higher coating hardness and increased surface roughness. Surface roughness values increased from about Ra 0.5 nm to Ra 4.3 nm as measured with XRR.⁵¹ The Si pin wear was significantly increased due to coating hardness and high surface roughness compared to amorphous TiO₂ (Table IV). The contact temperature was increased due to friction increase during sliding, further enhancing the oxide formation. Similar kind of tribolayer was formed when the bulk silicon pin was sliding against the uncoated silicon wafer, providing friction coefficient of 0.7. This is in the same range as the friction coefficient of many ALD films sliding against silicon. When a tribolayer was formed on the coating surface sliding against silicon pin, the contact occurred actually between similar materials (Si to Si) and due to this similarity the friction increased reaching similar friction values to silicon against silicon contact.

TABLE IV. Wear rates of the silicon pins and the ALD and reference coatings after 5 m continuous reciprocative sliding. The normal load was 0.3 N and the sliding velocity 0.01 ms⁻¹.

Counter material	Si pin wear rate (10 ⁻⁶ mm ³ /N m)	ALD coating wear rate (10 ⁻⁶ mm ³ /N m)
Si reference	970	a
100 nm 50 °C Al ₂ O ₃	850	a
300 nm 300 °C Al ₂ O ₃	790	a
100 nm 110 °C TiO ₂	120	a
100 nm 150 °C TiO ₂	410	a
100 nm 300 °C TiO ₂	1900	a
100 nm 110 °C ATO	6	b
100 nm 150 °C ATO	3	a
100 nm 250 °C ATO	140	a
100 nm 300 °C ATO	3	a
100 nm 300 °C PEALD TiN	<0.05	8
100 nm 400 °C TiAlCN	<0.05	70
100 nm 400 °C NbN	<0.05	2
85 nm DLC	<0.05	b

^aNot measurable due to tribolayer formation.

^bToo low wear to give a value.

For the ALD NbN coating, the tribolayer was formed on the silicon pin surface and no layer formation was observed on NbN coating. This behavior provided low friction performance in the range of 0.3 to 0.4 in the 5 m sliding tests. Also, the PEALD TiN film had the low friction value of 0.3 in the end of the sliding tests. Some measurable coating wear was detected on both TiN and NbN films with more occurring on NbN than TiN (Table IV).

The ALD TiAlCN coatings had similar tribolayer formation on the silicon pin as NbN, but the friction of TiAlCN coating reached values in the range of 0.4 to 0.6 in the end of the tests. The wear of the TiAlCN coating was high, since after 5 m sliding test, the coating was locally worn through, and after 20 m sliding, most of the coating was worn out. The SEM-EDS analyses of the tribolayer formed on the silicon pin proved that the layer consisted mostly of oxidized coating material, which showed the transfer of worn coating material onto the silicon surface.

In the long-term performance of 20 m sliding tests, PEALD TiN and ALD NbN had the lowest friction around 0.3–0.35 as presented in Fig. 8. In this case, the coatings experienced some wear and the tribolayer was formed on the silicon pin surface instead of the coating surface with a low amount of pin wear. Taking the adhesion problem of PEALD TiN into account, the NbN coating provided the best tribological performance with low friction and wear in the 20 m sliding tests in this study.

When comparing the friction performance of ALD films with the a-C:H type DLC coating, there was a clear difference in the performance. In the beginning of the tests, the friction of DLC films was between 0.2 and 0.3, but as the sliding proceeded, the friction was reduced and the DLC films provided low friction coefficient around 0.1 during 5 m sliding tests. No tribolayer formation was observed in this case. This friction performance is typical for the a-C:H coatings, and the results were in line with the published ones for a-C:H films sliding against different counterpart materials.⁵²

The low and stable friction performance is beneficial in most applications. For MEMS devices, besides DLC coating, ALD NbN and PEALD TiN could provide low friction performance. The wear of the Si pin and the thin film greatly influence the usability of the material pair in MEMS environment. The film materials, such as a-C:H, ALD NbN, and PEALD TiN, that have the wear rate of the pin and the film under 10^{-6} mm³/N m are more likely to provide satisfactory performance.

V. CONCLUSIONS

Tribological tests were carried out with silicon counterpart sliding against various ALD thin films, simulating the contacts occurring in the MEMS devices. In the tribological tests, the formation of the tribolayer in the contact area was the dominating phenomenon for friction and wear performance of ALD films. For the Al₂O₃, TiO₂, and ATO nanolaminate coatings, the tribolayer formation was observed with friction values stabilizing between 0.5 and 0.7. The TiAlCN film had friction values in the range of 0.4–0.6 in the end of the test and increased wear occurred on the coating. The

NbN and PEALD TiN coatings had lower friction in the range of 0.3–0.4. TiN suffered to some extent from wear and inadequate adhesion. The NbN film provided the most favorable friction and wear performance of the ALD films, yet lower friction was measured for the DLC a-C:H coating.

ACKNOWLEDGMENTS

The authors are grateful for Tekes—the Finnish Funding Agency for Innovation, ASM Microchemistry Oy, Beneq Oy, Murata Electronics Oy, Picosun Oy, Okmetic Oyj, and Oxford Instruments Analytical Oy for funding this work carried out in MECHALD project. Special thanks to Okmetic Oyj for providing bulk silicon for manufacturing the silicon pins used in the tribological experiments. Simo Varjus and Saima Ali are acknowledged for their contribution concerning tribological measurements and XRR, respectively. This work is linked to the Finnish Centres of Excellence in Atomic Layer Deposition (Reference No. 251220). L.K. designed the tribological experiments together with H.R. and performed the tribological experiments together with A.V. under supervision of H.R. R.L.P. and O.M.E.Y. were responsible for designing the ALD sample series. O.M.E.Y. made the Al₂O₃, TiO₂ and ATO growth at VTT. V.R. made the NbN growth at Aalto University; J.M. and T.S. made the 50 °C Al₂O₃ growth at University of Jyväskylä; X.L. and E.H. made nanoindentation measurements under supervision of S.P.H.; M.B. made the PEALD TiN growth; and M.T. made the TiAlCN growth. L.K. interpreted the data and wrote the literature review under supervision of H.R. and R.L.P. S.S. made XRR measurements and analysis under supervision of H.L. Co-authors discussed the results with L.K. and commented on the manuscript at all stages.

¹R. L. Puurunen, *J. Appl. Phys.* **97**, 121301 (2005).

²M. Ritala and M. Leskelä, *Handbook of Thin Film Materials*, edited by H. S. Nalwa (Academic, San Diego, CA, 2001), Vol. 1, pp. 103–159.

³S. M. George, *Chem. Rev.* **110**, 111 (2010).

⁴E. Ahvenniemi *et al.*, *J. Vac. Sci. Technol., A* **35**, 010801 (2017).

⁵R. L. Puurunen, H. Kattelus, and T. Suntola, *Handbook of Silicon Based MEMs Materials and Technologies*, edited by V. Lindroos, M. Tilli, A. Lehto, and T. Motooka, (Elsevier, Oxford, 2010), pp. 433–446.

⁶T. M. Mayer, J. W. Elam, S. M. George, P. G. Kotula, and R. S. Goeke, *Appl. Phys. Lett.* **82**, 2883 (2003).

⁷N. D. Hoivik, J. W. Elam, R. J. Linderman, V. M. Bright, S. M. George, and Y. C. Lee, *Sens. Actuator, A* **103**, 100 (2003).

⁸C. F. Herrmann, F. W. DelRio, D. C. Miller, S. M. George, V. M. Bright, J. L. Ebel, R. E. Strawser, R. Cortez, and K. D. Leedy, *Sens. Actuator, A* **135**, 262 (2007).

⁹T. W. Scharf, S. V. Prasad, T. M. Mayer, R. S. Goeke, and M. T. Dugger, *J. Mater. Res.* **19**, 3443 (2004).

¹⁰J. Kynäräinen *et al.*, *Sens. Lett.* **5**, 126 (2007).

¹¹R. L. Puurunen, J. Saari-Lahti, and H. Kattelus, *ECS Trans.* **11**, 3 (2007).

¹²M. Blomberg, H. Kattelus, and A. Miranto, *Sens. Actuator, A* **162**, 184 (2010).

¹³A. Rissanen, U. Kantojärvi, M. Blomberg, J. Antila, and S. Eränen, *Sens. Actuator, A* **182**, 130 (2012).

¹⁴R. L. Puurunen *et al.*, *Sens. Actuator, A* **188**, 240 (2012).

¹⁵B. D. Davidson, D. Seghete, S. M. George, and V. M. Bright, *Sens. Actuator, A* **166**, 269 (2011).

¹⁶K. Petersen, *Proc. IEEE* **70**, 420 (1982).

¹⁷K. E. Bean and P. S. Gleim, *Proc. IEEE* **57**, 1469 (1969).

¹⁸Q. Chen and G. Carman, “Microscale tribology (friction) measurement and influence of crystal orientation and fabrication process,” in

- Proceedings of the 13th Annual International Conference on Micro Electro Mechanical System* (2000), pp. 657–661.
- ¹⁹P. Stempflé and J. Takadoum, *Tribol. Int.* **48**, 35 (2012).
- ²⁰D. J. Fonseca and M. Sequera, *Int. J. Qual. Stat. Reliab.* **2011**, 820243 (2011).
- ²¹Y. Huang, A. S. S. Vasan, R. Doaraiswami, M. Osterman, and M. Pecht, *IEEE Trans. Device Mater. Reliab.* **12**, 482 (2012).
- ²²Z. Chai, X. Lu, and D. He, *Surf. Coat. Technol.* **207**, 361 (2012).
- ²³V. Ageh, H. Mohseni, and T. W. Scharf, *Surf. Coat. Technol.* **237**, 241 (2013).
- ²⁴V. Ageh, H. Mohseni, and T. W. Scharf, *Surf. Coat. Technol.* **241**, 112 (2013).
- ²⁵H. Mohseni and T. W. Scharf, *Wear* **332–333**, 1303 (2015).
- ²⁶T. W. Scharf, S. V. Prasad, M. T. Dugger, P. G. Kotula, R. S. Goeke, and R. K. Grubbs, *Acta Mater.* **54**, 4731 (2006).
- ²⁷C. Cannaro, J. Chinn, and B. Kobrin, “Exceptional wear resistance of MEMS devices coated with carbon-doped alumina films,” in *Proceedings of Solid-State Sensors, Actuators and Microsystems Conference*, Lyon, France (2007), pp. 1319–1320.
- ²⁸B. Kobrin, R. Nowak, and J. D. Chinn, “Wear-resistant, carbon-doped metal oxide coatings for MEMS and nanoimprint lithography,” U.S. patent US20100068489A1 (18 March 2010).
- ²⁹A. Erdemir and C. Donnet, *J. Phys. D: Appl. Phys.* **39**, 331 (2006).
- ³⁰C. Donnet and A. Erdemir, *Tribology of Diamond-Like Carbon Films—Fundamentals and Applications* (Springer, New York, 2008), p. 664.
- ³¹H. Ronkainen, S. Varjus, J. Koskinen, and K. Holmberg, *Wear* **249**, 260 (2001).
- ³²H. Ronkainen and K. Holmberg, “Environmental and thermal effects on the tribological performance of DLC coatings,” in *Tribology of Diamond-Like Carbon Films*, edited by C. Donnet and A. Erdemir (Springer, New York, 2008), pp. 155–200.
- ³³W. Kern, *Handbook of Semiconductor Wafer Cleaning Technology—Science, Technology, and Applications*, edited by W. Kern (William Andrew/Noyes, Westwood, NJ, 1993), pp. 1–67.
- ³⁴O. M. E. Ylivaara *et al.*, *Thin Solid Films* **552**, 124 (2014).
- ³⁵O. M. E. Ylivaara *et al.*, *J. Vac. Sci. Technol., A* **35**, 01B105 (2017).
- ³⁶V. Rontu, “Atomic layer deposition of niobium nitride thin films,” Master’s thesis (Aalto University, Espoo, Finland, 2014).
- ³⁷K. N. Stoev and K. Sakurai, *Spectrochim. Acta, B* **54**, 41 (1999).
- ³⁸S. Sintonen, A. Saima, O. M. E. Ylivaara, R. L. Puurunen, and H. Lipsanen, *J. Vac. Sci. Technol., A* **32**, 01A111 (2014).
- ³⁹L. G. Parratt, *Phys. Rev.* **95**, 359 (1954).
- ⁴⁰W. C. Oliver and G. M. Pharr, *J. Mater. Res.* **7**, 1564 (1992).
- ⁴¹D. C. Miller, R. R. Foster, S.-H. Jen, J. A. Bertrand, S. J. Cunningham, A. S. Morris, Y.-C. Lee, S. M. George, and M. L. Dunn, *Sens. Actuator, A* **164**, 58 (2010).
- ⁴²J. F. Shackelford, Y.-H. Han, S. Kim, and S.-H. Kwon, *CRC Materials Science and Engineering Handbook*, 4th ed. (CRC Press, Boca Raton, 2015), p. 371.
- ⁴³X.-J. Chen *et al.*, *Proc. Natl. Acad. Sci. U. S. A.* **102**, 3198 (2005).
- ⁴⁴A. Maxwell, S. Owen-Jones, and N. M. Jennett, *Rev. Sci. Instrum.* **75**, 970 (2004).
- ⁴⁵J. J. Worthman and R. A. Evans, *J. Appl. Phys.* **36**, 153 (1965).
- ⁴⁶A. C. Fischer-Cripps, *Nanoindentation* (Springer-Verlag, New York, 2011), pp. 1–19.
- ⁴⁷S. Oktay, Z. Kahraman, M. Urgen, and K. Kazmanli, *Appl. Surf. Sci.* **328**, 255 (2015).
- ⁴⁸L. Kilpi, O. M. E. Ylivaara, A. Vaajoki, J. Malm, S. Sintonen, M. Tuominen, R. L. Puurunen, and H. Ronkainen, *J. Vac. Sci. Technol., A* **34**, 01A124 (2016).
- ⁴⁹K. Holmberg, *Finnish J. Tribol.* **28**, 16 (2009), available at <https://journal.fi/tribologia/issue/view/3260/23>.
- ⁵⁰K. Holmberg and A. Matthews, *Coatings Tribology*, 2nd ed. (Elsevier, Oxford, 2009), p. 54.
- ⁵¹J. Lyytinen *et al.*, *Wear* **342–343**, 270 (2015).
- ⁵²A. Erdemir and J. M. Martin, *Superlubricity* (Elsevier, Amsterdam, 2007), pp. 253–294.